Conformational and Electronic Properties of a Microperoxidase in Aqueous Solution: A Computational Study

Carla Di Teodoro,[a, b] Massimiliano Aschi,*[a] Andrea Amadei,[c] Danilo Roccatano,[d] Francesco Malatesta,[e] and Luca Ottaviano[b]

A theoretical study of the conformational properties of a small heme peptide in aqueous solution is carried out by classical, long-timescale molecular dynamics simulations. The electronic properties of this species, that is, the relative energies of its excited electronic states and the redox potential, are reproduced and related to the conformational behavior using the perturbed matrix method and basic statistical mechanics. Our results show an interesting coupling between the conformational transitions and the electronic properties. These investigations, beyond the biophysically relevant results addressing the long-standing question of the actual role of the enzyme structure on the enzyme activity, are also of some methodological interest since they offer a further computational perspective for incuding the electronic degrees of freedom into the modeling of rather complex molecular systems.

1. Introduction

Microperoxidases (MP) are small heme peptides consisting of one or more short polypeptide chains covalently linked to an iron protoporhyrin IX moiety via thioether bonds, obtained by the proteolytic digestion of cytochrome c. In the last years, MP received great attention due to two reasons. First, MP are supposed to retain the gross structural features of the parent protein and a deep understanding of its physicochemical properties would therefore provide a breakthrough in the intimate knowledge of the effects of the protein matrix on the heme moiety. Second, it was shown that they can be plausibly employed in a huge number of applications (e.g., hystochemistry, electrochemistry, medicinal chemistry, and biosensor science). For these reasons, MP have been largely investigated both experimentally[1–6] and theoretically.[7–10]

Recently, some of us have undertaken a systematic study of an MP from *marinobacter hydrocarbonoclasticus*, MMP-5 (Figure 1), to experimentally investigate its electronic properties both in aqueous solution and absorbed over metal substrates.[11,12] From such studies MMP-5 shows rather interesting electronic features which are in line with similar MP.[2] Upon absorption over metal surfaces, the spectroscopic and electric behavior of MMP-5 appears rather different from strictly related systems lacking of peptide side chains. This result suggests a plausible crucial role of the aminocidic substituents beyond the simple structural characterization.[12] In aqueous solution, the UV/Vis spectrum results strongly pH-dependent.[11,13] This observation has been explained by considering that the fifth and sixth coordination position of MMP-5 is sensitive to the pH value. At physiological pH values one water molecule and the histidine moiety (His), via its imidazole side chain (see Figure 1), conceivably give rise to a high-spin coordination to the iron porphyrin center. At higher pH values other potential ligands, raising upon the deprotonation of the acidic sites

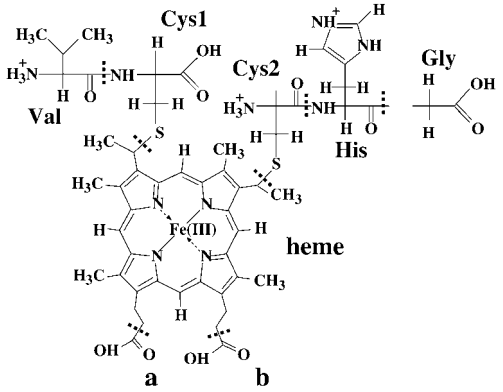

Figure 1. *Schematic view of MMP-5 at acidic conditions (note that the two water molecules coordinated to the iron center have been disregarded for the sake of clarity).*

[a] *C. Di Teodoro, M. Aschi*
Dipartimento di Chimica, Ingegneria Chimica e Materiali
Università dell'Aquila, via Vetoio 10, 67010 l'Aquila (Italy)
Fax: (+39) 0862-433-753
E-mail: aschi@caspur.it

[b] *C. Di Teodoro, L. Ottaviano*
Dipartimento di Fisica, Università dell'Aquila
via Vetoio 10, 67010 l'Aquila (Italy)

[c] *A. Amadei*
Dipartimento di Scienze e Tecnologie Chimiche
Università di Roma Tor Vergata, Roma (Italy)

[d] *D. Roccatano*
International University Bremen School of Engineering and Science
Campus Ring I, 28579 Bremen (Germany)

[e] *F. Malatesta*
Dipartimento di Biologia di Base ed Applicata
Università dell'Aquila, via Vetoio 10, 67010 l'Aquila (Italy)

 DOI: 10.1002/cphc.200400493

present in the side chains, can in principle bind the iron ion competing with His and water. The change of the ligand field, induced by this ligand exchanges, is therefore supposed to induce the high-to-low spin transition which could in principle induce sharp spectroscopic changes. This hypothesis, however, has never been quantitatively confirmed. A computational investigation of the electronic properties of aqueous MMP-5 at different pH values, would be therefore of great help. However, usual theoretical approaches could be in principle frustrated by the complexity of the system, that is, the presence of the water solvent, the presence of highly fluctuating side chains and, finally, the conceivable simultaneous existence of a large number of isomers.

In this respect, we have recently proposed[14,15] and successfully applied[16–18] a new computational approach, perturbed matrix method (PMM), particularly designed, through the combination of molecular dynamics (MD) simulations and quantum-chemical calculations, to address the electronic properties of complex molecular systems such as MMP-5. Herein, with the use of this theoretical-computational approach, we will try to address the study of aqueous MMP-5 essentially focussing on two basic questions: what does the MMP-5 structure look like, that is, the conformational features of the polypeptide chains in aqueous solution? Do the polypeptide chains have an effect on the electronic properties of the heme moiety? These two questions are, of course, mutually related and for their answer some points have to be clarified. As already remarked, the structure of the MMP-5 is strongly pH-dependent, at the same time, classical MD simulation require a well-defined topology of the molecular system.[19] Therefore, a complete and exhaustive MD-based study of MMP-5 should consider separately all the different isomers whose weight, at different pH values, should be carefully evaluated based on thermodynamic arguments.

In this first study we have limited our attention on the MMP-5 at acidic conditions, pH 1.5 (Figure 1), in which because of the full protonation of all the basic sites, no changes in the molecular covalent frame are expected to take place. Extentions of the present results at higher pH values are currently in progress in our laboratories.

This Article is organized as follows: in the first part the MD simulation will be described and its results will be used for addressing the conformational analysis of MMP-5. In the second part, with the use of PMM two important electronic properties of aqueous MMP-5, that is, its UV/Vis spectrum and its redox potential, will be evaluated and connected to the conformational properties previously studied.

Theoretical and Computational Methods

The main body of the theoretical basis of PMM is widely described in our previous articles.[14,15,18] Herein, only the main features of the computational strategy will be therefore outlined. The underlying philosophy of PMM is essentially in line with all the currently employed quantum mechanical/molecular mechanics (QM/MM) procedures. In other words, a portion of a complex molecular system, hereafter called quantum center (QC), herein the heme moiety, is treated quantum-mechanically with the rest of the system, in this case the peptide side chains and the solvent molecules, considered as a classical perturbation. The novelty in PMM is the way in which this perturbation is dynamically coupled to the QC. In fact, being $\mathbf{r}_n$ the nuclear coordinates of the QC and $\mathbf{x}$ the coordinates of the atoms providing the (classical) perturbing field, we can write, within certain approximations, the electronic (perturbed) Hamiltonian for the QC according to Equation (1)

$$\tilde{H}(\mathbf{r}_n,\mathbf{x}) \cong \tilde{H}^0(\mathbf{r}_n) + q_T V(\mathbf{r}_0,\mathbf{x})\tilde{I} + \tilde{Z}_I(\mathbf{E}(\mathbf{r}_0,\mathbf{x}),\mathbf{r}_n) + \Delta V(\mathbf{r}_n,\mathbf{x})\tilde{I} \quad (1)$$

where $\tilde{H}^0(\mathbf{r}_n)$ is the unperturbed Hamiltonian matrix which can be constructed by a standard electronic structure calculation on the QC in vacuo, $V(\mathbf{r}_0,\mathbf{x})$ and $\mathbf{E}(\mathbf{r}_0,\mathbf{x})$ are the (perturbing) electric potential and the electric field at a given QC $\mathbf{r}_0$ position (typically the geometrical center), $\tilde{Z}_I(\mathbf{E},\mathbf{r}_n)$ is the perturbation energy matrix explicitly given by $[\tilde{Z}_1]_{I,I'} = -\mathbf{E}\cdot\langle\Phi_I^0|\hat{\boldsymbol{\mu}}|\Phi_{I'}^0\rangle$ and $\Delta V(\mathbf{r}_n,\mathbf{x})$ approximates the perturbation due to all the higher-order terms as a simple short range potential.[15,18] Φ_I^0 are the unperturbed Hamiltonian eigenfunctions obtained by the quantum-chemical calculations in vacuo, which provide the basis set for expressing all the matrices used. If an MD simulation or, more generally, a conformational space sampling is carried out, a sequence of $\mathbf{E}$ and V is therefore produced. Hence, the diagonalization of $\tilde{H}(\mathbf{r}_n,\mathbf{x})$, carried out along the configurational sampling will produce a trajectory of perturbed eigenvalues ε_i and eigenvectors $\mathbf{c}_i$ of the QC and, therefore, a trajectory of whatever perturbed electronic properties. Extracting the perturbed excitation energies and the related perturbed transition dipoles $\boldsymbol{\mu}_{ij} = \langle\Phi_i|\hat{\boldsymbol{\mu}}|\Phi_j\rangle$, where $\boldsymbol{\mu}_{ij}$ is evaluated by Equations (2)–(5),

$$\mu_{ij} = \mathbf{c}_i^{*T}\tilde{\Lambda}_x^0\mathbf{c}_j\mathbf{i} + \mathbf{c}_i^{*T}\tilde{\Lambda}_y^0\mathbf{c}_j\mathbf{j} + \mathbf{c}_i^{*T}\tilde{\Lambda}_z^0\mathbf{c}_j\mathbf{k}$$

$$[\tilde{\Lambda}_x^0]_{I,I'} = \langle\Phi_I^0|\hat{\mu}_x|\Phi_{I'}^0\rangle \quad (2)$$

$$[\tilde{\Lambda}_y^0]_{I,I'} = \langle\Phi_I^0|\hat{\mu}_y|\Phi_{I'}^0\rangle \quad (3)$$

$$[\tilde{\Lambda}_z^0]_{I,I'} = \langle\Phi_I^0|\hat{\mu}_z|\Phi_{I'}^0\rangle \quad (4)$$

we can readily obtain by a straightforward statistical averaging, the electronic vertical excitation distribution corrected by the transition probability, that is, the electronic spectrum without the internal quantum vibrational contribution.

The curve for the $i \rightarrow j$ transition, denoted by $I_{i,j}(\lambda)$, can be obtained using Equation (6), where $B_{i,j}$ is the Einstein coefficient calculated by Equation (7), combined with the probability density $\rho(\lambda)$ of excitation in the wavelength λ space (i.e., the probability to find the chromophore within a given excitation energy interval divided by the corresponding λ interval), both as obtained by MD simulation and PMM:

$$I_{i,j}(\lambda) = B_{i,j}\rho(\lambda) \quad (6)$$

$$B_{i,j} = \frac{|\mu_{i,j}|^2}{6\varepsilon_0\hbar^2} \quad (7)$$

The perturbed transition dipole $\boldsymbol{\mu}_{i,j}$ is calculated by averaging within a given λ interval. Note that in the previous equations, we have assumed a unitary density of the electromagnetic radiation. The first essential step of our study is therefore the MD simulation of the entire system. At this purpose, we used the Gromacs software package.[20] A time step of 1 fs with the isokinetic temperature coupling was adopted.[21] A cut-off radius of 1.0 nm for the short-range interactions and the particle mesh Ewald (PME) method for the long-range electrostatics was employed.[22] All the bond lengths were constrained using the SHAKE algorithm.[23] The

roto-translational constraint was also imposed to the solute (the MMP-5 molecule) both to speed-up the water molecule relaxation and to obtain the correct thermodynamics and statistical mechanics.[24] The simulated system was described by the Gromos 96[25] force field with the atomic charges of the heme moiety recalculated[26] for simulating the sextet state, that is, the actual ground state of the MMP-5. Note that only the polar hydrogen atoms have been explicitly included. The following simulation procedure was employed:

1) We have constructed a simulation box with a 27-nm^3 volume consisting of one MMP-5 molecule, kept fixed at its center,[27] single point charge (SPC) water molecules and four chloride counterions.[28] The starting structure of MMP-5 was taken from the crystal structure of *marinobacter hydrocarbonoclasticus* dimeric cytochrome c.[29] The dimension of the box was carefully selected for a correct application of the periodic boundary conditions.
2) A steepest descent minimization of the solution followed by an MD simulation in an *NPT* ensemble with the MMP-5 fixed, was performed for equilibrating the solvent molecules.
3) The whole system was slowly heated from 50 to 300 K.
4) Finally, an MD was carried out in the canonical (*NVT*) ensemble at 300 K for 67.5 ns.

Essential dynamics (ED) analysis was performed over the equilibrated portion of the trajectory using the Gromacs software and some of our own routines.[30] In a second step we have to evaluate the unperturbed basis set of the QC for the application of PMM. At this purpose, quantum calculations have been performed using the Gamess package.[31]
The heme moiety, with the two coordinate water molecules, (hereafter indicated as Fe^{III}P

1) From the equilibrated portion of the MD simulation we extracted the average conformation of QC.
2) A structural relaxation was carried out at the Hartree–Fock level of theory using a mixed atomic basis set (hereafter termed as BSI) consisting of a (6s,3p)/
3) All magnetic states of Fe^{III}P
4) The DFT vectors, optimized as described in the previous point, were finally used for carrying out configuration interaction calculations, including all the single and double excitations (CISD) with an active space consisting of nine electrons in 12 orbitals.

This quantum-chemical calculation provided the unperturbed basis set, consisting of the ground and 19 excited states, for the PMM application. The same computational procedure was applied also for the quintet state of Fe^{II}P

2. Results and Discussion

2.1 Conformational Behavior of Aqueous MMP-5

We initially focus our attention on the structural properties of MMP-5 in aqueous acidic solution. To qualitatively establish when the system reaches the equilibrium condition, we have evaluated along the trajectory the root-mean-square deviation (RMSD) with respect to the starting structure, whose time course is reported in Figure 2. The RMSD curve shows that the system, after an initial long drift of 22.1 ns, reaches a plateau

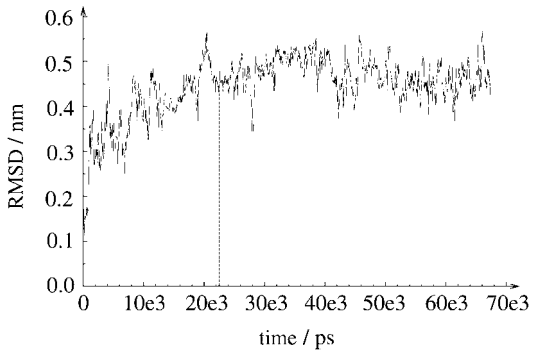

Figure 2. *Root-mean-square deviation of all atoms of MMP-5 with respect to the starting structure.*

at 0.47 ± 0.04 nm. It is important to underline that even for this relatively small system, a long-timescale MD simulation is necessary for ensuring an exhaustive and significant sampling of the phase space.

To characterize the internal motions of MMP-5, we have evaluated the root-mean-square fluctuation (RMSF) of the equilibrated portion of the trajectory. These results are reported in Figure 3. Not surprisingly, the peptide side chains as well as the propionate groups result as the most fluctuating portion of the molecule. On the other hand, as already observed in our previous study, the Fe^{III}P

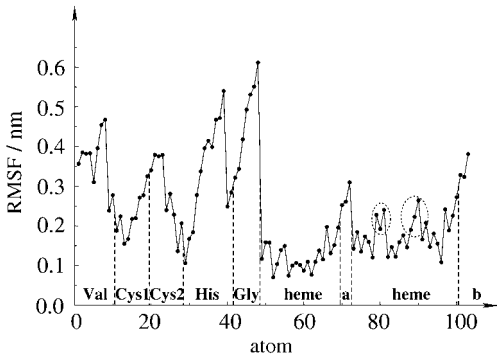

Figure 3. *Root-mean-square fluctuation of all atoms of MMP-5 along the equilibrated portion of the trajectory. The circled portions refer to the methyl groups connected to the Cys residues. For the nomenclature used, refer to Figure 1.*

Moreover, we also carefully checked the relative positions of the four chloride counterions with respect to the MMP-5 molecule. From this analysis, at least along the equilibrated portion of the trajectory, none of them is found to fall in the vicinity of the solute. This result is important for mimicking the high dilution conditions.

To better characterize the above-mentioned large amplitude motions and, in particular, for describing in more detail the conformational equilibria of MMP-5, we carried out an essential dynamics analysis.[30] This procedure allows to separate the intramolecular large collective (essential) motions, basically responsible for the conformational transitions, from the remaining small amplitude, that is, near-constrained fluctuations. At

this purpose using the positional fluctuations of all atoms belonging to the MMP-5, since no roto-translational motions are present in our simulation, a covariance matrix was constructed and diagonalized, providing a new set of generalized coordinates which correspond to the eigenvectors of the matrix itself. Each eigenvector represents the direction in the configurational space associated with the largest fluctuation, that is, the largest eigenvalue in the space defined by the eigenvector itself and the remaining ones, that is, with smaller eigenvalues. From the spectrum of the eigenvalues and the related normalized cumulative fluctuation, both shown in Figure 4 and in the inset, respectively, the first two eigenvectors turn out to account for almost 60 percent of the overall fluctuations. In the same inset we also roughly describe the nature of these essential eigenvectors. The first one crudely corresponds to a correlated movement of the two peptide side chains. The second one involves the Cys-His-Gly chain and the opposite propionate group indicated with **a** (Figure 4) in an anticorrelated movement. It is important to note that the long peptide

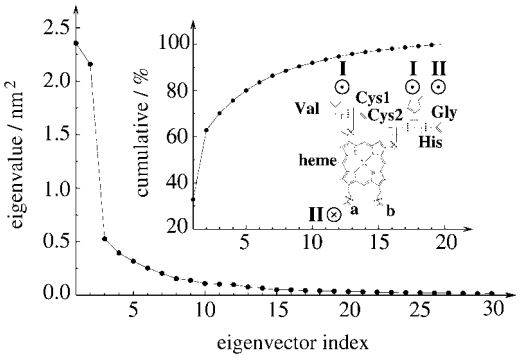

Figure 4. *Spectrum of the eigenvalues from the diagonalization of the covariance matrix carried out along the equilibrated portion of the trajectory. In the inset are also shown the cumulative fluctuations and the schematic description of the first two essential eigenvectors denoted as I (described by two arrows pointing outside the plane indicating the correlated movement of the involved peptide chains) and II (using the same representation adopted for the first eigenvector the two arrows describe the anticorrelated motion involving the corresponding chains).*

chains do not experience any movement toward the heme moiety and always appear as almost completely stretched. Therefore, we have projected the trajectory on the plane defined by this two eigenvectors obtaining a set of points that provide the sampling of the conformational space.

This procedure hence allows an evaluation of all thermodynamics associated to the conformational sampling of the MMP-5. In other words, on the essential plane previously defined we can locate the free-energy minima which basically correspond to the conformations actually sampled by MMP-5 in the simulated conditions. At this purpose, we have divided the essential plane in 5050 intervals and calculated the Helmholtz free-energy difference between an interval j and the reference interval i, $\Delta A_{i\rightarrow j}$, using Equation (8)

$$\Delta A_{i\rightarrow j} = -kT \ln \frac{\rho_j}{\rho_i} \qquad (8)$$

where k is the Boltzmann constant, T is the temperature and ρ_i, ρ_j are the probability of finding the system in a state j and in a reference state i corresponding to the state with the highest probability. In Figure 5 a three distinct free-energy minima,

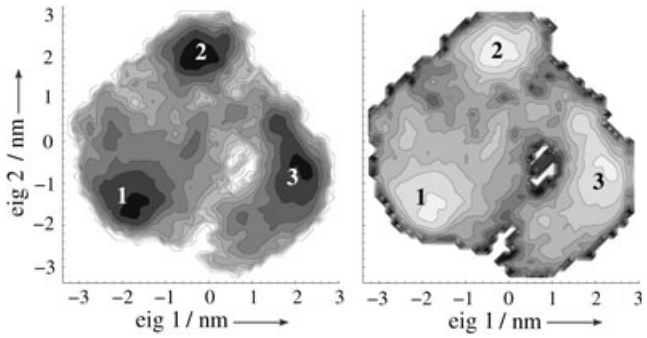

Figure 5. *Free-energy (left) and entropy (right) variation as a function of the two essential coordinates. Left: 1, 2, and 3 indicate the deepest free-energy minima. Free-energy minimum 2, lying at −19.97 kJ mol^{-1}, is the absolute minimum. Free-energy minima 1 and 3 are, respectively, 1.20 kJ mol^{-1} and 0.97 kJ mol^{-1} less stable than minimum 2. Right: Entropy maximum 2 is the absolute maximum. 1 and 3, lying at −3.7 J mol^{-1} K^{-1} and −3.6 J mol^{-1} K^{-1} with respect to 2, are local entropy maxima.*

that is, three distinct conformers, can be observed. The corresponding average structures are shown in Figure 6. All free-energy minima show some interestingly common features. As already observed from the analysis of the eigenvectors, in all

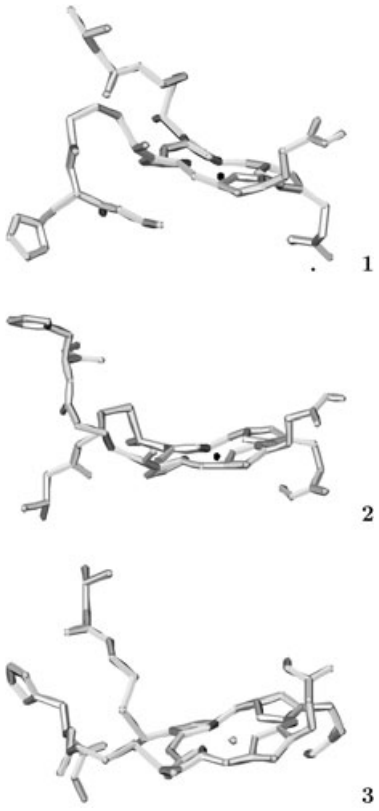

Figure 6. *Representative structures correponding to the free-energy minima 1, 2, 3 shown in Figure 5. Note that the two water molecules coordinated to the iron center, have been omitted for the sake of clarity.*

conformers the side chains systematically maintain far away from the heme moiety. This behavior can be qualitatively explained by reminding that, at the conditions selected for the simulation, the side chains are fully protonated and therefore they preferentially stay far away from the heme which is also positively charged. At a more detailed inspection none of the above-mentioned structures was found to be characterized by specific close contacts suggesting intramolecular interactions, for example, hydrogen bonds. This latter observation therefore stimulates the obvious question how the above-mentioned free-energy minima can be rationalized. We have hence evaluated both the contribution of the internal energy and of the entropy. The calculation of this last quantity is straightforward using Equation (9)

$$\Delta S_{i\rightarrow j} = \frac{1}{T}(\Delta U_{i\rightarrow j} - \Delta A_{i\rightarrow j}) \quad (9)$$

where $\Delta U_{i\rightarrow j}$ is the total potential energy, directly obtained by the simulation. In Figure 5 (right), where $\Delta S_{i\rightarrow j}$ is shown, we can interestingly observe three entropy maxima at the same position of the free-energy minima. On the other hand, the internal energy (not reported) results almost flat in this space. This latter observation can be qualitatively explained by considering that the MMP-5 experiences essentially the same interactions when the side chains are exposed to the solvent, that is, water, or when they internally interact. Our findings, therefore indicate that the aqueous MMP-5 at low pH values is a system in which the conformational sampling is entropically driven. This result certainly deserves further accurate analysis to evaluate which factors can be related to the entropy increase. At this purpose, one should evaluate, along the same essential plane, the extent of the fluctuation pattern on the whole system, that is, MMP-5, water molecules and counterions. Due to the strong difficulties associated to this analysis we decided to limit such an evaluation only to a qualitative observation of the change of the fluctuation pattern of some structural features, such as peptide chains, their own side chains, the propionate groups, and water molecules. In particular, within the peptide chains, we also monitored the fluctuation of the dihedral angles which are a direct indication of their internal mobility. From our analysis, it turns out that all of the above-mentioned groups do contribute to the entropy increase. As a matter of fact, the two peptide chains undergo a sharp increase, corresponding to the entropy maxima, of their fluctuation around the C–S bonds. At the same time, also the side chains (which include all the peptide atoms not belonging to the backbone) do experience a strong increment of their own fluctuation. The role of the propionate group **a,** whose maximal internal mobility coincides with the maxima 2 and 3 in Figure 5, results to be not negligible. Finally, we also evaluated the extent of the solvent molecule fluctuation by monitoring the effect of their fluctuating electric field on the geometrical center of the heme moiety. This last quantity turned out to be more easily accessible than the direct measure of the fluctuation on the essential plane. From this analysis, which is not explicitly reported for the sake of brevity, we could identify a relatively strong electric field fluctuation corresponding to the entropy maximum 2.

2.2 UV/Vis Spectrum of Aqueous MMP-5

In our previous studies carried out both on large macromolecules and small solutes, PMM has proven to be a rather efficient tool for evaluating the coupling between the conformational motions and the electronic properties of the QC. Therefore, also in this case we try to investigate if this effect is present. However, first it is important to evaluate the validity of our model. At this end, we try to reproduce the experimental UV/Vis spectra of aqueous MMP-5. In particular we have considered the spectrum region corresponding to the Soret band, experimentally located at about 390 nm, that is, 3.18 eV. Moreover, we also investigated the 500–700-nm region in which three weak signals are typically monitored: the Q_V band (λ_{max} at 520 nm = 2.38 eV), the Q_0 band (λ_{max} at 560 nm = 2.21 eV) and the charge-transfer (CT) band (λ_{max} at 620 nm = 2 eV).

As already explained in the previous section, for calculating all these spectra we have used Equations (6) and (7). Since Fe^{III} can exist in three different magnetic states (doublet, quartet, sextet) none of them should in principle be disregarded for a complete modelization of the spectrum. However, our unperturbed calculations showed that the sextet state turned out to be, by far, most stable. Therefore, on the basis of this result and considering that—also experimentally—this state is the only one detected at low pH values for MMP-5 [13] and for other structurally similar MP,[2,35] we performed PMM calculations only on this magnetic state.

Before showing the PMM results it is important to remark that from the analysis of our unperturbed CISD/BSI calculations, in the region around 390 nm, several transitions (from $0\rightarrow10$ to $0\rightarrow16$) are actually present, all of them showing the same $\pi\rightarrow\pi^*$ character.[36] Consequently, for correctly evaluating the real Soret band, all above-mentioned transitions have been taken into account.

The final spectrum, shown in Figure 7, was calculated by simply adding all transitions since they did not result to be degenerate. The maximal intensity, centered at about 355 nm (3.49 eV), is in satisfactory agreement with the experimental

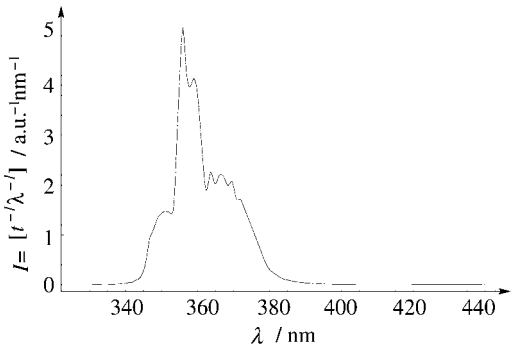

Figure 7. *Calculated absorbtion spectrum in the region between 350–400 nm (Soret band). The y axis shows the intensity [I(λ)] calculated by Equation (6);* t = *time in [a.u.] and λ in [nm].*

value (3.18 eV). Note that the difference of 0.31 eV between the theoretical and the experimental results is within the limit of the chemical accuracy of the unperturbed calculations (CAUC).[37] At this point, we evaluated the effect of the fluctuations of the electric field produced by the molecular environment (peptide chains, propionate groups and solvent molecules) on the energy and intensity of the Soret band. This effect should be independently evaluated on all electronic transitions defining this band.

However, we only considered the transitions which resulted most intense in the presence of the perturbation, that is, the 0→13, the 0→14 and the 0→15 transitions.

To have a first qualitative indication about the differential effect of the solvent and the peptide chains, we report in Table 1 the peak maxima λ_M of the three transitions and the peaks maxima obtained removing the perturbation of peptide and propionate chains (λ_M^{solv}) and the same peaks obtained removing the perturbation of the solvent (λ_M^{chain}). Note that this comparison is carried out in the same ensemble (aqueous MMP-5).

Table 1 shows that the solvent and the peptide chains provide two opposite contributions: a shift of the unperturbed maximum toward the blue (the solvent) and a shift toward the red (the peptide chains). Consequently the actual spectrum raises from a combination of these effects.

Table 1. *Comparison of the calculated absorbtion maxima of the aqueous MMP-5 (λ_M), with the absorbtion maxima and without the effect of the peptide and propionate chains (λ_M^{solv}), with the absorbtion maxima and without the effect of the solvent (λ_M^{chain}) and with the absorbtion maxima of the QC in vacuo (λ_M^{unp}).*

0→i	λ_M [eV]	λ_M^{solv} [eV]	λ_M^{chain} [eV]	λ_M^{unp} [eV]
0→13	3.39	3.49	3.22	3.45
0→14	3.48	3.64	3.39	3.48
0→15	3.50	3.67	3.45	3.55

If compared to our previous studies, this result is, in some way, a novelty.[16,17] In fact when we were dealing with an enzyme, the solvent field had only a limited and indirect role concerning the perturbation of the transitions. More precisely, the solvent was normally found to play the role of modulating the fluctuation of the protein whose field is, on the other hand, mainly responsible for the perturbation. In this case, it has to be remarked that the MMP-5 has relatively short peptide chains which cannot completely surround the QC. Moreover, we should also consider that such chains, from the previous conformational analysis, are found to be always completely stretched, favoring the access of the solvent molecules in the vicinity of the QC.

Finally, we addressed the search for a correlation between the conformational motions of the chains and the spectral properties. More precisely, our first aim is to evaluate, if a direct correlation exists between the conformational minima and the transition energies and momenta.

At this purpose, we have projected the perturbed transition energies and momenta, that is, λ and μ^2, on the first two eigenvectors, labelled as λ_j and μ_j^2 ($j=1,2$). This procedure allows a direct estimation of the modulation of $\lambda_j(\mu_j^2)$ induced by the conformational changes of the MMP-5. It is obvious that a clear coupling between $\lambda_j(\mu_j^2)$ and these slow motions could be definitely only assumed if the extent of this modulation [indicated as $\Delta\Lambda_j$ (ΔM_j^2)] is significantly larger than the standard deviation for each value of $\lambda_j(\mu_j^2)$. In Figure 8 we have reported

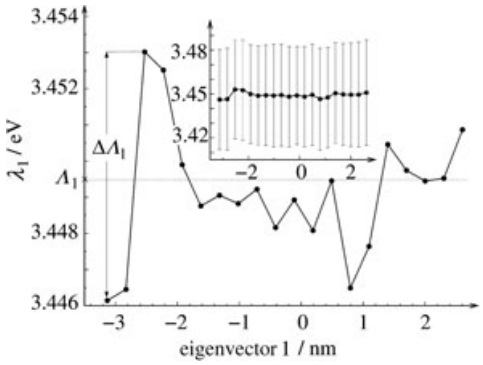

Figure 8. *Projection of the excitation energy (λ_1) for the 0→14 transition. The parameters $\Delta\Lambda_1$ and Λ_1, collected in Table 2, are also schematically shown. In the inset we report the same curve with the relative standard deviations.*

the λ values for the 0→14 transition as a function of the first eigenvector. For the sake of brevity, the results concerning other transitions are reported in Table 2.

It clearly emerges that the essential motions do not appreciably modify the excitation energies and momenta. In fact, from Table 2, the dispersion of λ and μ^2 ($\Delta\Lambda_j$ and ΔM_j^2) invariably appears lower than the related standard deviations. This result clearly indicates that we cannot establish any correlation between the conformational transitions and the spectral properties.

Table 2. *Analysis of the perturbing field effect on the absorbtion wavelength and the dipole of the Soret transition. Λ_j and M_j ($j=1, 2$) are the central values, of the wavelength and of the transition dipole, respectively, from the projection along the jth eigenvector. $\Delta\Lambda_j$ and ΔM_j are their dispersions and $\overline{\left(\frac{\Delta\lambda_j}{\lambda_j}\right)}$ and $\overline{\left(\frac{\Delta\mu_j^2}{\mu_j^2}\right)}$ are the average standard dispersions.*

0→i	Λ_1 [eV]	$(\Delta\Lambda)_1$ [%]	$\overline{\left(\frac{\Delta\lambda_1}{\lambda_1}\right)}$ [%]	Λ_2 [eV]	$(\Delta\Lambda)_2$ [%]	$\overline{\left(\frac{\Delta\lambda_2}{\lambda_2}\right)}$ [%]
0→13	3.39	0.34	1.68	3.38	0.47	1.67
0→14	3.45	0.20	1.0	3.45	0.25	1.0
0→15	3.35	0.30	0.97	3.52	0.2	0.97
0→i	M_1 [a.u.]	$(\Delta M^2)_1$ [%]	$\overline{\left(\frac{\Delta\mu_1^2}{\mu_1^2}\right)}$ [%]	M_2 [a.u.]	$(\Delta M^2)_2$ [%]	$\overline{\left(\frac{\Delta\mu_2^2}{\mu_2^2}\right)}$ [%]
0→13	1.52	7.60	49.7	1.53	6.70	49.6
0→14	0.82	13.60	82.0	0.81	22.1	81.9
0→15	0.73	9.68	92.0	0.71	20.4	92.0

Finally we analyzed the 500–700 nm spectral region. Three peaks, reported in Figure 9, were found with their maxima centered at 506 nm (2.45 eV, the Q_V), at 562 nm (2.21 eV, the Q_0) and at 680 nm (1.82 eV, the CT). These signals, as also experimentally observed, showed low intensities which prevent a quantitative comparison with the experimental values. It can be only qualitatively argued that, if compared to the corresponding experimental maxima previously reported and also considering CAUC in this case, our results are in good agreement.[13] We also briefly remark that a similar analysis, carried out on these transition, again does not reveal any appreciable coupling with the conformational fluctuations.

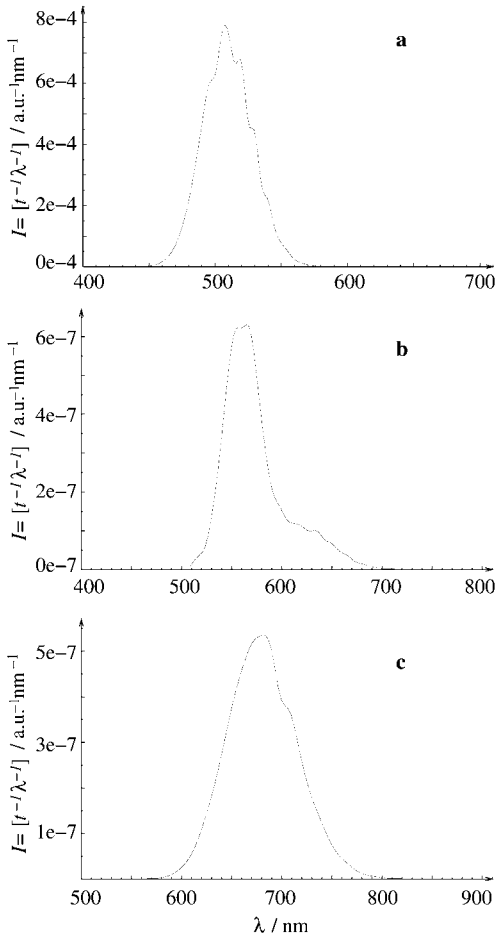

Figure 9. *Calculated absorption spectra in the visible region. a) Q_V, b) Q_0 and c) CT. The y axis shows the intensity [I(λ)] calculated by Equation (6); t = time in [a.u.] and λ in [nm].*

In conclusion, the band width in all spectra is entirely ascribed to the solvent flucuations and to the near-constrained (low eigenvalues) fluctuations. The application of PMM provides rather good results for reproducing complicated observables such as the absorbtion spectrum of a highly fluctuating molecule in solution. However, unlike the heme in protein environment,[16,17] the relative ground-excited states electronic properties of MMP-5 in aqueous solution are not modulated by the conformational fluctuations of the molecular environment. This observation plausibly indicates some intrinsic differences emerging when this species is within its natural environment and when it is in aqueous solution.

2.3 Toward a Modelization of the Electrochemical Properties of MMP-5

Apart from the spectral calculations we have used PMM to study also another important property of MMP-5. It is well-known that MP are involved in several electron transfer processes.[2] Therefore, it could be of great fundamental and practical interest to understand in detail its electrochemical properties whose theoretical modelization is, however, a problem of tremendous complexity.[38] Consequently, in this last section, we wish to focus our attention only on the semireaction given in Equation (10)

$$\text{MMP-5(III)} + 1e^- \rightarrow \text{MMP-5(II)} \qquad (10)$$

where (III) and (II) indicate the presence of Fe^{III} and Fe^{II}, respectively.

Equation (10) is the first step for a complete investigation of a real electrochemical environment. In particular, we addressed the effects of peptide and propionate chains as well as of the solvent fluctuations on the free energy associated to the above-mentioned redox process.

Although no experimental values are available for MMP-5, several measurements, carried out at low pH values for similar peroxidases, can provide a reliable reference for our calculations.[2]

For systems where the oxidation state of the QC does not alter the internal energy of the environment, as in typical simulation where nonpolarizable force fields are used, the free-energy change associated to the semi-redox reaction [Eq. (10)], assuming no modification of the quantum-vibrational energies, is calculated using Equations (11) and (12)

$$\Delta A^{\ominus} = -kT \ln\langle e^{-\beta\Delta\varepsilon}\rangle_{(III)} \qquad (11)$$

where

$$\Delta\varepsilon = \varepsilon_{(II)} - \varepsilon_{(III)} \qquad (12)$$

is the electronic ground-state energy change due to the redox process.

We evaluated the unperturbed electronic properties of the sextet heme (Fe^{III}) and the quintet heme (Fe^{II}) moieties in their ground state at the B3LYP/BSI level as described in the Computational Methods Section. Subsequently, using the MMP-5(III) trajectory, PMM was applied to obtain the perturbed electronic energy of the two oxidation states, that is, $\varepsilon_{(III)}$ and $\varepsilon_{(II)}$. It is worth to note that all the calculations were performed using the potential energy minima of the $FeP(H_2O)_2$ in both oxidation states (Fe^{III} and Fe^{II}).

However, for Fe^{II} the presence of a stable QC pentacoordinate geometry with a single water molecule and the iron center significantly placed out of the porphyrin ring is also

possible.[17] Such latter geometry has not been considered herein as these calculations require an independent further simulation which will be addressed in forthcoming studies. Note also that the calculations of the free energy associated to the process given in Equation (10) were carried out using Equation (11), implicitly assuming that the average is performed over the statistical ensemble of MMP-5(III). Consequently, our result approximate the actual redox potential as much as the thermodynamic weight of the pentacoordinate complex can be neglected and, also, as much as the statistical ensemble of the oxidized state resembles the statistical ensemble of the reduced state. Of course, at this stage, we cannot evaluate the weight of the above-mentioned factors.

The $\Delta A^{\ominus}$ is calculated from the trajectory. To evaluate the standard redox potential $V^{\ominus}$, we need to calculate the standard free energy $\Delta A^{\ominus}_{H_3O^+/H_2}$ of the reference reaction [Eq. (13)], which allows the use of Equation (14):

$$H_3O^+_{(sol)} + 1e^- \rightarrow \frac{1}{2}H_{2(g)} + H_2O_{(l)} \quad (13)$$

$$V^{\ominus} = -\frac{1}{F}(\Delta A^{\ominus} - \Delta A^{\ominus}_{H_3O^+/H_2}) \quad (14)$$

where F is the Faraday constant. The results are reported in Table 3.

Table 3. *Calculated values for the unperturbed $Fe^{III}P(H_2O)_2/Fe^{II}P(H_2O)_2$ electronic energies from DFT calculations ($\Delta\varepsilon^0$). $\Delta\varepsilon$ is the average perturbed $Fe^{III}P(H_2O)_2/Fe^{II}P(H_2O)_2$ electronic energy, $\Delta A^{\ominus}$ is the free energy of the reaction given in Equation (10) according to Equation (11), $\sigma_{\Delta A^{\ominus}}$ is the related standard deviation, $\Delta A^{\ominus}_{H_3O^+/H_2}$ is the free energy of the reference semi-reaction and $V^{\ominus}$ is the calculated redox potential of MMP-5.*

$\Delta\varepsilon^0$	$\Delta\varepsilon$	$\Delta A^{\ominus}$	$\Delta A^{\ominus}_{H_3O^+/H_2}$	$\sigma_{\Delta A^{\ominus}}$	$V^{\ominus}$
−6.92 eV	1.66 eV	0.38 eV	0.02 eV	0.07 eV	−450 mV

We can observe from the unperturbed ($\Delta\varepsilon^0$) and perturbed ($\Delta\varepsilon$) electronic energy that an inversion of the stability takes place, when the perturbation of the molecular environment acts over the QC. In vacuo the electronic energy of heme(II) is much lower than that of heme(III).

Interestingly, the calculated redox potential, −450 mV, is of the same order of magnitude as the experimental values for similar MPs, suggesting that probably the above-mentioned drawbacks, that is, the use of a hexacoordinate Fe^{II} complex and the Fe^{III} statistics are not severe.[2]

The large difference between the average energy ($\Delta\varepsilon$) and the free energy ($\Delta A^{\ominus}$) for the semi-reaction [Eq. (10)] is remarkable.

This apparently strange result can be easily explained by the observation of a large fluctuation of the the difference between the ground state of heme(III) and heme(II) along the trajectory. Consequently, in some parts of the trajectory this difference decreases significantly. This behavior of the energy fluctuation justifies the dramatic decrease of $\Delta A^{\ominus}$ and, in physical terms, indicates that in some parts of the trajectory the electron migration can be facilitated (of course that happens if an oxidant species of the MMP-5 is present).

This fluctuation can be almost entirely ascribed to the heme(III) ground-state perturbed energy oscillation. In fact, the time course of the heme(II) perturbed energy shows a rather low fluctuation.

Finally, in analogy to the UV/Vis analysis, we focussed our attention on the existence of a correlation between $\Delta A^{\ominus}$ and the conformational fluctuations, postulated for a long time and in a large number of theoretical papers.[38] Therefore, the electron-transfer free energy has been calculated as a function of the first two essential eigenvectors, exactly using the same procedure adopted to obtain Figure 5. The result shown in Figure 10 indicates that, unlike the spectral properties of the MMP-5, three distinct minima emerge and they correspond to the conformational free-energy minima [Figure 5 (left)].

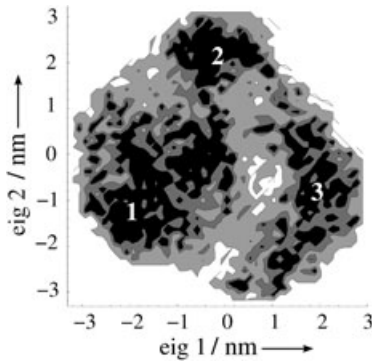

Figure 10. *Free energy of the semireaction [MMP-5 reduction, Equation (10)] as a function of the essential coordinates. The black regions correspond to more negative values of the redox potential*

This result confirms that the molecular environment fluctuations, strongly modulating this important property, cannot be neglected for a reliable theoretical modelization of the electron transfer in condensed phase. A final comment deserves the difference observed between the UV/Vis electronic properties and the electron transfer process.

In the first case the effect of the perturbation acts on the same quantum center [MMP-5(III)] and the fluctuation of the perturbed energies, involved in electronic transitions, turned out to be rather similar. On the other hand, as already remarked in the case of the electron transfer reaction, the response of the two partners to the electric perturbation resulted quite different, producing a free-energy landscape much more corrugated.

3. Conclusions

Herein, the conformational and related electronic properties of the MMP-5 in acidic aqueous solution have been investigated by means of classical molecular dynamics simulations and quantum-chemical calculations. The emerged picture shows that, rather interestingly, the conformational behavior of this

molecule is entropically driven. As a matter of the fact, the conformational minima sampled by MMP-5 correspond to portion of the configurational space in which the fluctuation of the peptide and propionate groups as well as of the solvent molecules are maximized. The application of the PMM has also provided a rather good reproduction of the most important UV/Vis signals of MMP-5 in acidic aqueous solution indicating, at the same time, the lack of any relevant correlation between these spectroscopic quantitites and the conformational fluctuations. On the other hand, this correlation has been observed to play a key role in modulating the free energy for the MMP-5(III) reduction, suggesting the importance of the molecular environment on the electrochemical properties of this species.

Our study further confirms the reliability and the capability of PMM in describing the electronic properties of complex molecular systems at the equilibrium.

Acknowledgements

This work was partially supported by Programma di Ricerca Scientifica Interuniversitario Nazionale "Bioenergetica: Aspetti Genetici, Biochimici e Fisiopatologici" (PRIN 2003) from MIUR, Italy. We gratefully acknowledge Prof. Alfredo Di Nola (University of Roma "La Sapienza") for stimulating discussions and for providing some of the computational facilities. We also acknowledge Dr. Lorenzo Caputi.

Keywords: electron transfer · electronic excitation · molecular dynamics · photochemistry · solvent effects

[1] F. Nastri, A. Lombardi, L. D Andrea, M. Sanseverino, O. Maglio, V. Pavone, *Biopolymers* **1998**, *47*, 5-22.
[2] R. A. Scott, A. Grant Mauk, *Cytochrome C: A Multidisciplinary Approach*, U. S. B., Sausalito, California, **1996**.
[3] S. K. Chapman, S. Da , A. W. Munro in *Structure and Bonding*, Springer Verlag, Berlin, Heidelberg, **1997**, *88*, pp. 39-70.
[4] D. A. Baldwin, H. M. Marques, J. M. Pratt, *J. Inorg. Biochem.* **1987**, *30*, 203-217.
[5] J. W. Owens, C. J. O Connor, *Coord. Chem. Rev.* **1988**, *84*, 1-45.
[6] R. Ippoliti, A. Picciau, R. Santucci, G. Antonini, M. Brunori, *Biochem. J.* **1997**, *328*, 833-840.
[7] H. M. Marques, K. L. Braun, *Coord. Chem. Rev.* **2002**, *225*, 123-158.
[8] S. Melchionna, M. Barteri, G. Ciccotti, *J. Comput.-Aided Mol. Des.* **1995**, *2*, 9.
[9] G. Ranghino, G. Antonini, P. Fantucci, *Isr. J. Chem.* **1994**, *34*, 239.
[10] S. Melchionna, M. Barteri, G. Ciccotti, *J. Phys. Chem.* **1996**, *100*, 19241.
[11] L. Caputi, L. Di Leandro, A. Di Tullio, F. De Angelis, F. Malatesta, *J. Biol. Chem.* submitted.
[12] C. Di Teodoro, *PhD Thesis*, Università di l'Aquila, **2005**.
[13] L. Caputi, F. Malatesta, unpublished results.
[14] M. Aschi, R. Spezia, A. Di Nola, A. Amadei, *Chem. Phys. Lett.* **2001**, *344*, 374-380.
[15] R. Spezia, M. Aschi, A. Di Nola, A. Amadei, *Chem. Phys. Lett.* **2002**, *365*, 450-456.
[16] R. Spezia, M. Aschi, A. Di Nola, M. D. Valentin, D. Carbonera, A. Amadei, *Biophys. J.* **2003**, *84*, 2805-2813.
[17] M. Aschi, C. Zazza, R. Spezia, C. Bossa, A. Di Nola, M. Paci, A. Amadei, *J. Comput. Chem.* **2004**, *7*, 974.
[18] A. Amadei, C. Zazza, M. D Abramo, M. Aschi, *Chem. Phys. Lett.* **2003**, *381*, 187.
[19] With the term topology we are refering to the description of the covalent connectivities characterizing the molecular system.
[20] H. J. C. Berendsen, D. van der Spoel, R. van Drunen, *Comput. Phys. Commun.* **1995**, *91*, 43.
[21] D. J. Evans, G. P. Morriss, *Statistical Mechanics of Nonequilibrium Liquids*, Academic Press, London, **1990**.
[22] T. A. Darden, D. M. York, L. G. Pedersen, *J. Chem. Phys.* **1993**, *98*, 10089.
[23] J. P. Ryckaert, G. Ciccotti, H. J. C. Berendsen, *J. Comp. Physiol.* **1977**, *23*, 327.
[24] A. Amadei, G. Chillemi, M. A. Ceruso, A. Grottesi, A. Di Nola, *J. Chem. Phys.* **2000**, *112*, 9-23.
[25] W. F. van Gunsteren, S. R. Billeter, A. A. Eising, P. H. Hünenberger, P. Krüger, A. E. Mark, W. R. P. Scott, I. G. Tironi, *Biomolecular Simulation: The GROMOS96 Manual and User Guide*, Hochschulverlag AG an der ETH Zürich, Zürich, **1996**.
[26] The atomic charges were calculated using the CHelpG protocol[27] on an unrestricted Hartree–Fock optimized wavefunction carried out with the Huzinaga basis set.
[27] C. M. Breneman, K. B. Wiberg, *J. Comput. Chem.* **1990**, *11*, 361.
[28] K. A. Feenstra, B. Hess, H. J. C. Berendsen, *J. Comput. Chem.* **1999**, *20*, 786-798.
[29] A. Ilari, G. Colotti, L. Federici, L. Di Leandro, F. Malatesta, *Ital. J. Biochem.* **2002**, *51*, 104.
[30] A. Amadei, A. B. M. Linssen, H. J. C. Berendsen, *Proteins* **1993**, *17*, 412.
[31] M. W. Schmidt, K. K. Baldridge, J. A. Boatz, S. T. Elbert, M. S. Gordon, J. J. Jensen, S. Koseki, N. Matsunaga, K. A. Nguyen, S. Su, T. L. Windus, M. Dupuis, J. A. Montgomery, *J. Comput. Chem.* **1993**, *14*, 1347.
[32] S. Huzinaga in *Gaussian Basis Sets for Molecular Calculations*, Elsevier, Amsterdam, **1984**.
[33] A. Schafer, H. Horn, R. Ahlrichs, *J. Chem. Phys.* **1992**, *97*, 2571.
[34] A. D. Becke, *J. Chem. Phys.* **1993**, *98*, 5648.
[35] D. W. Low, H. B. Grey, J. O. Duus, *J. Am. Chem. Soc.* **1997**, *119*, 1-5.
[36] Strictly speaking, we cannot rigorously define for the heme moiety as a π–π^* orbital. We have therefore considered such orbitals on the basis of lower symmetry elements (molecular plane) and the weight of single atoms in their definition.
[37] For a definition of chemical accuracy, see for example: J. A. Pople, M. Head-Gordon, D. J. Fox, K. Raghavachari, L. A. Curtiss, *J. Chem. Phys.* **1989**, *90*, 5622.
[38] D. Dominguez-Ariza, C. Hartnig, C. Sousa, F. Illas, *J. Chem. Phys.* **2004**, *121*, 1066, and references therein cited.

Received: October 15, 2004

